

Polymer Chemistry

Accepted Manuscript



This is an *Accepted Manuscript*, which has been through the Royal Society of Chemistry peer review process and has been accepted for publication.

Accepted Manuscripts are published online shortly after acceptance, before technical editing, formatting and proof reading. Using this free service, authors can make their results available to the community, in citable form, before we publish the edited article. We will replace this *Accepted Manuscript* with the edited and formatted *Advance Article* as soon as it is available.

You can find more information about *Accepted Manuscripts* in the [Information for Authors](#).

Please note that technical editing may introduce minor changes to the text and/or graphics, which may alter content. The journal's standard [Terms & Conditions](#) and the [Ethical guidelines](#) still apply. In no event shall the Royal Society of Chemistry be held responsible for any errors or omissions in this *Accepted Manuscript* or any consequences arising from the use of any information it contains.

ARTICLE

Hexylthiophene Side Chained
4,7-di-2-thienyl-2,1,3-benzothiadiazole and Benzodithiophene
based Copolymer for Efficient Organic Solar Cells<res://XDict.exe/word.html>

- ##Cite this: DOI:

10.1039/x0xx00000x

Junzhen Ren^{a,b†}, Xichang Bao^{b†}, Liangliang Han^b, Jiuxing Wang^b, Meng Qiu^b,
Qianqian Zhu^b, Tong Hu^{a,b}, Ruiying Sheng^{a,b}, Mingliang Sun^{a*}, Renqiang Yang^{b*}.

Received 00th January 2012,

Accepted 00th January 2012

DOI: 10.1039/x0xx00000x

www.rsc.org/

In this work, hexylthiophene substituted thiophene-bridge is used to connect benzodithiophene (BDT) and benzothiadiazole (BT) segment to build new photovoltaic polymer (PBDT-DTTBT). The highest occupied molecular orbital (HOMO) level of the polymer is decreased by 0.2 eV to be -5.47 eV compared to the reference polymer without hexylthiophene side chain, which may be ascribed to the conformational torsion caused by the steric hindrance from the bulky hexylthiophene side group. The band gap of the polymer shows no obvious change with the same backbone polymer without hexylthiophene side chain (around 1.7 eV). Polymer solar cells (PSCs) based on PBDT-DTTBT and [6,6]-phenyl-C₇₁-butyric acid methyl ester (PC₇₁BM) exhibit a power conversion efficiency (PCE) of 6.19% with an open-circuit voltage (V_{oc}) of 0.80 V, a short-circuit current density (J_{sc}) of 12.72 mA·cm⁻² and a fill factor (FF) of 60.97%. The work provides a new method to design new conjugated polymers with a deep HOMO level and low band gap for high V_{oc} PSCs.

Introduction

Bulk-heterojunction (BHJ) polymer solar cells (PSCs) have attracted tremendous attentions in the past decade, owing to their distinctive potentials for fabricating light-weight, large-area and flexible devices by low-cost roll-to-roll processing technique.¹⁻⁴ Recently, power conversion efficiency (PCE) over 10% have been achieved for both single and tandem solar cells.^{2, 5-11} But ideal polymer materials are still needed for their further commercialization.¹² To obtain high PCE, photovoltaic polymers should be designed under consideration of varies of factors, such as high hole mobility, suitable molecular energy levels, broad absorption and decent solubility.¹³⁻¹⁶ To harvest more solar energy, low band-gap (LBG) conjugated polymers should be designed and synthesized. Using alternative donor-acceptor (D-A) structures to design the backbones of LBG polymers has become the most popular and successful strategy.¹⁷⁻¹⁹ By the rational selection and optimization of D-A building blocks to hybridize the frontier orbital of the electron-rich units (donors) and the electron-deficient units (acceptors), the band gaps of the polymers can be effectively tuned, as well as the molecular energy levels and optical properties.²⁰⁻²³

As is well-known, PCE is a product of short-circuit current density (J_{sc}), open-circuit voltage (V_{oc}) and fill factor (FF). V_{oc} is proportional to the energy level difference between the highest occupied molecular orbital (HOMO) of the conjugated polymer and the lowest unoccupied molecular orbital (LUMO) of the fullerene, and thus a deeper HOMO level polymer is crucial to get higher V_{oc} .^{24, 25} Yang et al. did a systematic study on PBDTBzT-DTfBT with a PCE of 7.3% containing benzothienyl-substituted

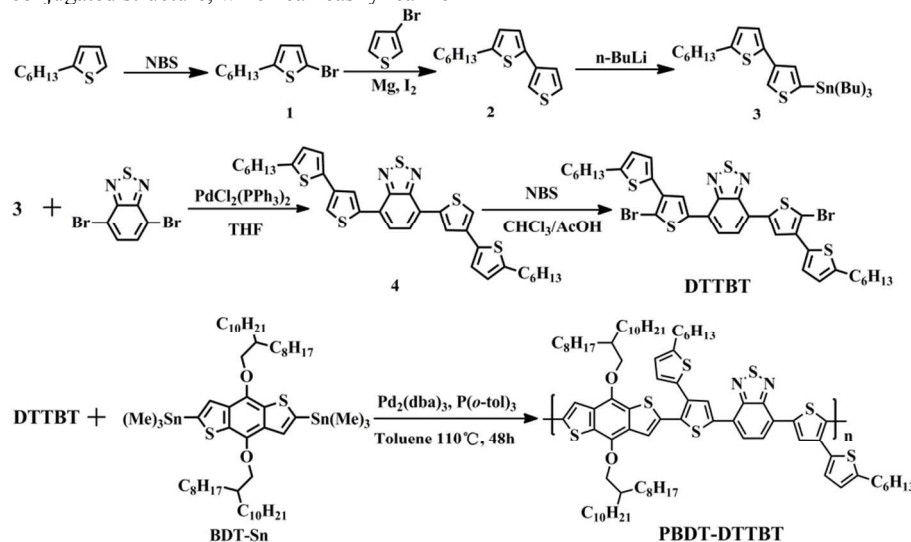
benzodithiophene (BDT), which has a deep HOMO level at -5.47 eV, corresponding to a V_{oc} of 0.9 V.²⁶ Huang et al. synthesized three polymers with a new acceptor unit of naphtho[1,2-c:5,6-c']bis(2-octyl[1,2,3]triazole) (TZNT), and realized the PCE of 7.1% with a high V_{oc} of 0.9 V.²⁷ Beaujuge et al. constructed the conjugated polymers PBDT(T)TPD(CO) polymerized from two-dimensional BDT with thieno[3,4-c]pyrrole-4,6(5H)-dione (TPD), and the device showed the high PCE of 6.7% with a high V_{oc} of 1.05 V.²⁸ In terms of these materials' structures, the design strategy of "weak donor" and "strong acceptor" were used, which led to deep HOMO energy levels, thereby increasing V_{oc} .²⁹ But in some case, by using strong acceptor to build high V_{oc} OPV material, the researchers have to accept the increased bandgap (E_g) and the resultant decreased J_{sc} .^{30,31}

Besides the approach of using strong acceptor, there are also some other ways to increase V_{oc} of OPV materials, such as the bulky side chain engineering. For classical polythiophene (PT) systems, the bulky groups as side chains were reported to show strong steric hindrance effect between bulky side groups and adjacent thiophene repeating units.³²⁻³⁴ The steric hindrance caused a large dihedral angle and thus the conjugated degree of the main chains decreased, consequently leading to a deep HOMO level. While the bulky side groups usually led to large band gaps and resultant low J_{sc} as the "weak donor" and "strong acceptor" strategy did.³⁴ Hsu et al. constructed a indacenodithiophene based polymer (PIDTHT-BT) with pendent n-hexylthiophene units.³⁵ By the conjugated side chains induced conformational twisting of PIDTHT-BT, a deep HOMO level was obtained. Compared with the PSCs device performance

based on PIDTDT-BT (indacenodithiophene polymer without *n*-hexylthiophene chain), the V_{oc} of on PIDTHT-BT based PSCs device increased by 0.2 V approximately and a high J_{sc} remained.

In this paper, to further explore the steric hindrance effect on the energy levels and E_g , we selected benzodithiophene (BDT) and benzothiadiazole (BT) as donor and acceptor building blocks, and introduced hexylthiophene substituent to the thiophene bridges between BDT and BT to construct the target polymer PBBDT-DTTBT. Compared to other donor units, such as indacenodithiophene, carbazole and fluorene, BDT unit has asymmetric and planar conjugated structure, which can easily realize

ordered π - π stacking with a large domain size.³⁶ As a rigid ring, thiophene has a larger volume than the alkyl chains. When attached to the main chains, the thiophene side chain can twist the polymer backbone for a deeper HOMO level. Moreover, strong electrostatic repulsion effect between electronegative sulfur atoms in the thiophene side chains and the adjacent BDT units, may further promote the torsion effect.³² The synthesized polymer exhibited a low-lying HOMO energy level of -5.47 eV, and an unchanged band gap of 1.7 eV, compared to other reported polymers with the same backbone.³⁷⁻⁴² By this method, the V_{oc} was increased by ~0.1 V, compared to the reference polymer PBBDT-DTBT, and a PCE of 6.19% is obtained.³⁷



Scheme 1 Synthetic route and molecular structure of PBBDT-DTTBT.

Results and discussion

The synthetic routes of the monomers and the target polymer are shown in Scheme 1. The experimental section displays the detailed experimental procedures for the synthesis of the monomers and the polymer, where DTTBT and BDT-Sn were synthesized according to previously reported methods.^{39, 43, 44} 5-Hexyl-2,3'-bithiophene was introduced to BT core by Stille coupling reaction using bis(triphenylphosphine)-palladium(II) chloride ($\text{PdCl}_2(\text{PPh}_3)_2$) as catalyst to construct compound 4. DTTBT was prepared with bromine in mixed solvent of chloroform and acetic acid. The polymer PBBDT-DTTBT was synthesized via Stille coupling polymerization between DTTBT and BDT-Sn in the presence of $\text{Pd}_2(\text{dba})_3$ and $\text{P}(o\text{-tol})_3$. The polymer can be readily dissolved in common organic solvents, such as chloroform, toluene and *o*-dichlorobenzene. The structure of the synthesized polymer was characterized by ^1H NMR. PBBDT-DTTBT polymer shows a number average molecular weight (M_n) of 54.93 kDa, a weight-average molecular weight (M_w) of 210.3 kDa, and a polydispersity index of 3.8, determined by gel permeation chromatography (GPC).

Thermal Stability

The thermal stability of the polymer was analyzed by thermo gravimetric analysis (TGA) with a heating rate of 10 °C/min under a

nitrogen atmosphere. The polymer has good thermal stability with decomposition temperatures at 340.7°C (5% weight loss) as shown in Figure 1. Obviously, the thermal stability of conjugated polymers is high enough for their application in PSCs. This high decomposition temperature can depress the deformation of the polymer/PCBM blend film morphology and the degradation of the blended active layer under applied electric fields in PSCs devices.³⁶

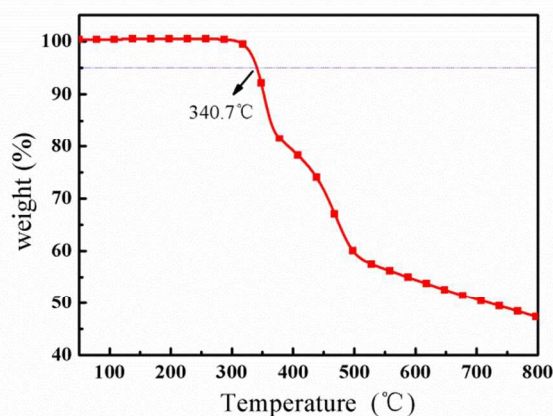


Figure 1. TGA curve of PBBDT-DTTBT.

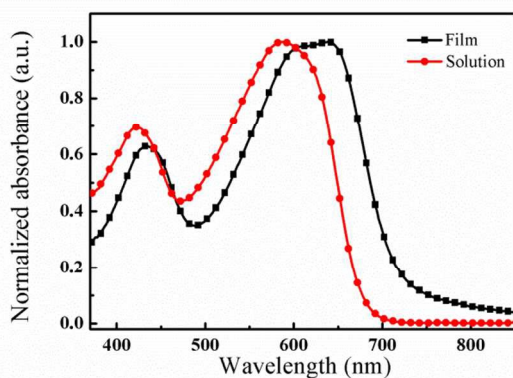


Figure 2. UV-vis absorption spectra of PBDT-DTTBT in dilute chloroform solution and in thin solid film.

Optical Properties

The ultraviolet-visible (UV-vis) absorption spectra of PBDT-DTTBT in dilute chloroform solution and in thin film on quartz substrate are shown in Figure 2. PBDT-DTTBT displays a broad absorption from ~400 nm to ~700 nm in solution, and two feature absorption bands are observed with the absorption peak located at 422 and 588 nm, corresponding to the localized π - π^* transitions of the polymer backbone and the intramolecular charge transfer (ICT) from the electron-donating BDT unit and thiophene bridge to the electron-accepting benzothiadiazole unit, respectively.⁴⁵⁻⁴⁷ As to the film, PBDT-DTTBT shows broader absorption and distinct red-shift compared to that in solution. The red-shift should be attributed to better planarity of the polymer with the extension of the conjugated structures and stronger electronic interaction between the polymer chains in the film state.^{48, 49} In addition, a shoulder peak located at 610 nm indicates strong intermolecular π - π^* stacking as a result of the aggregations of the polymer chains.^{45, 50} The absorption onset of PBDT-DTTBT film is at 718 nm, corresponding to an optical band gap (E_g^{opt}) of 1.73 eV. In addition, the polymer exhibits an absorption coefficient $5.1 \times 10^4 \text{ L mol}^{-1} \text{ cm}^{-1}$ in the CHCl_3 solution and an absorption coefficient $6.1 \times 10^4 \text{ cm}^{-1}$ in the thin solid film at the absorption peak (Figure S1), which is similar with the previously reported polymers.^{37,38,42}

Electrochemical Properties

Cyclic voltammetry (CV) was used to measure the electronic energy levels of the conjugated polymer. The HOMO level can be readily estimated from the onset oxidation potential in the cyclic voltammogram.⁵¹ The cyclic voltammogram of PBDT-DTTBT as film is shown in Figure 3. To obtain the oxidation potential of the polymer, the reference electrode was calibrated using ferrocene/ferrocenium (Fc/Fc⁺), which had a redox potential with an absolute energy level of -4.80 eV in vacuum; the potential of this external standard under the same conditions was 0.39 V vs saturated calomel electrode (SCE). As shown in Figure 3, the onset oxidation potential (E_{ox}) is 1.06 V vs SCE. According to the equation $E_{\text{HOMO}} = -e(E_{\text{ox}} + 4.8 - E_{1/2,(\text{Fc}/\text{Fc}^+)})$, the HOMO level of PBDT-DTTBT is -5.47 eV, which is a relative deep HOMO level among the alkyl

substituted BDT-DTBT polymers.³⁷⁻⁴² Here, the polymers with the 2D-BDT structure were excluded from this comparison table, because it has been suggested that the 2D structure can affect the HOMO levels and V_{oc} of PSCs devices.⁵² The deep HOMO should be attributed to the decreased degree of the π -orbital overlap along the main chains caused by strong steric interaction between the rigid thiophene side group and the adjacent BDT units. The interaction between the electronegative sulfur atoms in the conjugated side chains and the adjacent BDT units may further increase the distortion.³² The LUMO level is -3.74 eV, calculated from the equation $E_{\text{LUMO}} = E_{\text{HOMO}} + E_g^{\text{opt}}$, which is significantly higher-lying than that of PC₇₁BM (ca. -3.91 eV); thus, efficient exciton dissociation can be expected in the solar cells devices.⁵³

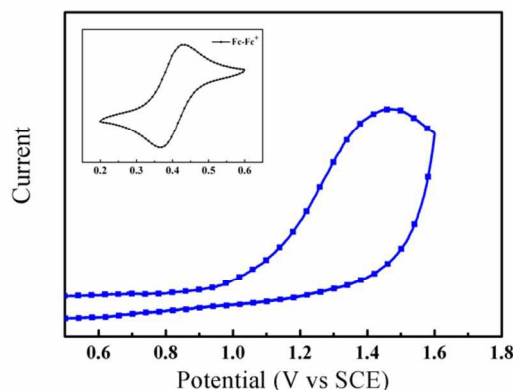


Figure 3. Cyclic voltammetry of PBDT-DTTBT.

The band gap, HOMO and LUMO energy levels of PBDT-DTTBT are listed in Table 3 in comparison with other five polymers with same backbones. It can be found that PBDT-DTTBT has a relatively deep HOMO level compared to the others, but the band gap is very similar with the other polymers (around 1.7 eV). The result shows that introducing hexylthiophene substituent to the thiophene bridges can simultaneously down-shift the HOMO and LUMO energy levels without changing band gap of the polymer.

Theoretical Calculations

To evaluate the impact of conformation torsion on molecular architecture and consequently on the optoelectronic properties of the polymers, density functional theory (DFT) calculations were performed by using the Gaussian 09 program at the B3LYP/6-31G(d,p) level in the gas phase. The optimized molecular geometries were confirmed to be minimum-energy conformations by computing vibrational frequencies at the same level. The dihedral angles, HOMO and LUMO energy levels, band gaps and corresponding electron distributions were calculated, where the counterpart polymer PBDTT-DTBT (without hexylthiophene substituent) was also calculated for comparison. To minimize the computation demand, the alkyl chains attached to BDT units and thiophene side groups were replaced by methyl groups in the calculation process. The molecule structure sketch used for computation is shown in Figure 4, where θ_1 is the dihedral angle

between BDT unit and thiophene bridge, θ_2 is the dihedral angle between thiophene bridge and BT unit, θ_3 is the dihedral angle between thiophene bridge and methylthiophene side group drawn in red. (Figure 4 and 5)

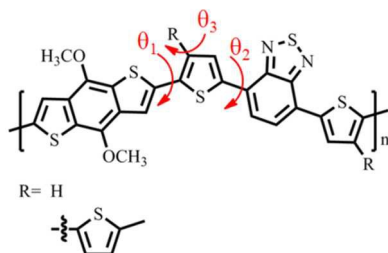


Figure 4. Molecular geometry sketch used for the DFT computation

Table 1. Calculated dihedral angles and corresponding HOMO, LUMO levels and bandgaps (E_g^{cal}) of PBBDT-DTBT and PBBDT-DTTBT

Polymer	θ_1 (deg)	θ_2 (deg)	θ_3 (deg)	HOMO (eV)	LUMO (eV)	E_g^{cal} (eV)
PBBDT-DTBT	5.60	0.2	-	-5.02	-2.74	2.28
PBBDT-DTTBT	35.6	6.7	59.1	-5.03	-2.71	2.32

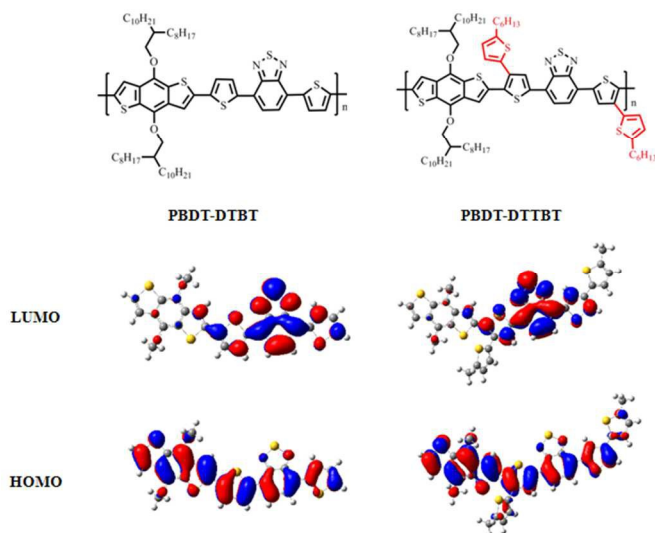


Figure 5. The frontier molecular orbital (HOMO and LUMO) obtained from DFT calculations for the polymer PBBDT-DTBT and PBBDT-DTTBT. Color code: gray (C), white (H), red (O), blue (N), and yellow (S).

As shown in Table 1, the dihedral angle θ_1 between BDT unit and thiophene bridge and θ_2 between thiophene bridge and BT unit of PBBDT-DTBT are 5.6° and 0.2° respectively, implying relatively planar conformation of PBBDT-DTBT. In contrast, PBBDT-DTTBT has obviously larger θ_1 and θ_2 compared to that of PBBDT-DTBT, which should be attributed to the strong steric hindrance of the

thiophene side groups caused conformation torsion. In this case, the π -orbital overlap between neighboring aromatic units are decreased, which may lead to changes in the frontier orbital energy levels. There is also a large dihedral angle θ_3 between methylthiophene side group and thiophene bridge, which implies large torsion between thiophene side group and thiophene bridge. And the large torsion leads to negligible π -orbital overlap between thiophene side group and the backbone, which is consistent with the calculated energy distribution shown in Figure 5. The distributions of the frontier molecular orbitals of the two polymers are similar, where the HOMO is delocalized over the whole backbone while the LUMO is mainly located in the BT units and thiophene bridges.

Photovoltaic Properties and Morphology Characterization

Table 2. Photovoltaic properties of the PSCs based on the blend of PBBDT-DTTBT and PC₇₁BM

Ratio (A : D)	DIO (%)	V_{oc} (V)	J_{sc} (mA/cm ²)	FF (%)	PCE _{max} /PCE _{ave} ^a
0	0	0.83±0.01	9.48±0.12	47.96±0.90	3.91/ (3.76±0.13)
1	0.81±0.01	12.08±0.15	58.20±0.87	5.67/ (5.66±0.01)	
1:1	2	0.80±0.01	12.56±0.22	60.38±0.70	6.19/ (6.05±0.16)
3	0.79±0.01	11.69±0.21	59.11±1.53	5.74/ (5.49±0.25)	
4	0.78±0.01	11.36±0.26	57.82±2.35	5.58/ (5.11±0.16)	

^a The average PCE was obtained from five devices.

To investigate the photovoltaic properties of PBBDT-DTTBT, BHJ PSCs devices with a structure of ITO/PEDOT:PSS/PBBDT-DTTBT:PC₇₁BM/Ca/Al were fabricated and characterized under the illumination of AM1.5G, 100 mW/cm² with different active layer thickness and donor-acceptor weight ratio, where the polymer was used as the electron donor and PC₇₁BM was used as the electron acceptor. (Table S1 and Figure S2) It was found that the optimized performance was achieved with the weight ratio of PBBDT-DTTBT:PC₇₁BM at 1:1 (w/w) and the thickness of the active layer at about 130 nm. According to many previously reported studies, a small amount of 1,8-diodooctane (DIO) can drastically enhance the interpenetrating nanoscale morphology, thus improving the PCE of PSCs for polymer/fullerene systems.⁵⁴⁻⁵⁶ So different ratios of DIO were added to the PBBDT-DTTBT:PC₇₁BM system to further improve the PCE of the devices, and the corresponding photovoltaic parameters of the devices with different contents of DIO are summarized in Table 2. Figure 6 shows the J - V curves and external quantum efficiency (EQE) of devices based on PBBDT-DTTBT/PC₇₁BM (1:1, w/w) blend films with DIO or not. Without any additives or post-treatments, a moderate PCE of 3.91%

was achieved with a V_{oc} of 0.83V, a J_{sc} of 9.48 mA/cm² and a FF of 47.96%. After processed with 2 v/v% DIO, the optimal PCE of 6.19% was obtained. Compared to the device without additive, the J_{sc} and FF values of the device with 2% DIO increased to 12.56 mA/cm² and 60.38%, respectively. The EQE with 2% DIO exhibits maximum value of 69%, which is higher than that without DIO (47%), and therefore DIO treated devices show higher J_{sc} .

The donor photon energy loss is defined as $E_g - eV_{oc}$, where E_g is the optical band gap of the donor polymer and V_{oc} is obtained

from the corresponding solar cell device with either PC₆₁BM or PC₇₁BM.^{23, 57} Here, the $E_g - eV_{oc}$ values of PBDT-DTTBT and the other analogs were calculated and shown in Table 3. The $E_g - eV_{oc}$ value of PBDT-DTTBT is 0.93 eV, which is close to other efficient PSCs materials PBDTHDO-DTHBTff (0.92 eV) and PBDTDTBT (0.93 eV). It implies hexylthiophene side chain can help the polymer to show good photovoltaic performance in the same backboned polymer analogs.

Table 3. Comparison molecular energy level data and photovoltaic properties of PBDT-DTTBT and the other analogs

Polymer ^a (D)	Acceptor (A)	HOMO (eV)	LUMO (eV)	E_g^{opt} (eV)	V_{oc} (V)	$E_g - eV_{oc}$ (eV)	J_{sc} (mA/cm ²)	FF (%)	PCE (%)	Ref.
PBDT-DTTBT	PC ₇₁ BM	-5.47	-3.74	1.73	0.80	0.93	12.56	60.38	6.19	This work
PBDT-DTBT	PC ₇₁ BM	-5.26	-3.50	1.72	0.70	1.02	10.43	62.00	5.01	37
PBDT-TBT-C8	PC ₇₁ BM	-5.29	-3.53	1.77	0.71	1.06	8.60	51.00	3.15	38
P(BDT-TT-BT)	PC ₇₁ BM	-5.21	-3.43	1.78	0.69	1.09	11.34	63.00	4.93	39
PBDTC ₆ DBT	PC ₇₁ BM	-5.21	-3.53	1.68	0.63	1.05	6.18	48.00	1.86	40
PBDT _{HDO} -DT _H BTff	PC ₇₁ BM	-5.31	-3.61	1.70	0.78	0.92	15.38	69.20	8.30	41
PBDTDTBT	PC ₇₁ BM	-5.24	-3.52	1.72	0.79	0.93	13.56	69.10	7.40	42

^a The molecular structures of PBDT-DTBT, PBDT-TBT-C8, P(BDT-TT-BT), PBDTC₆DBT, PBDT_{HDO}-DT_HBTff and PBDTDTBT are shown in Figure S3.

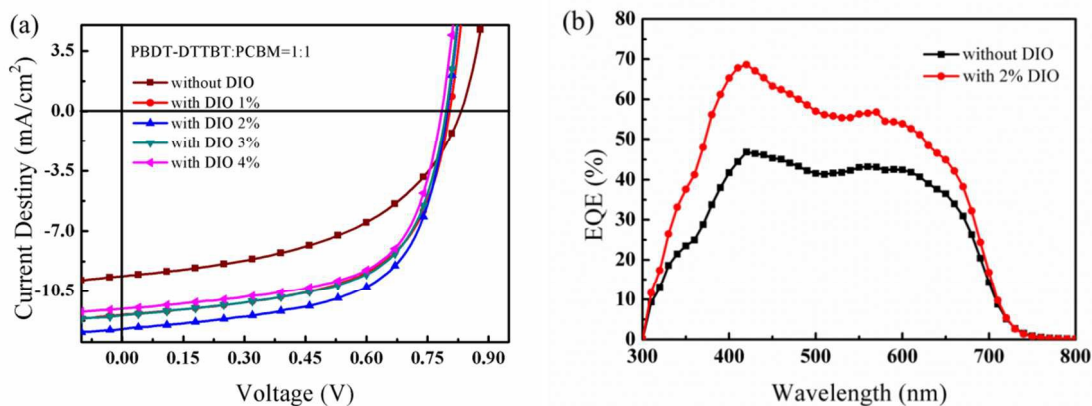


Figure 6. (a) J - V characteristics of PSCs based on the PBDT-DTTBT/PC₇₁BM blends spin-coated with different DIO content; (b) EQE of devices based on PBDT-DTTBT/PC₇₁BM (1 : 1, w/w) blend film with 2% DIO or not.

ARTICLE

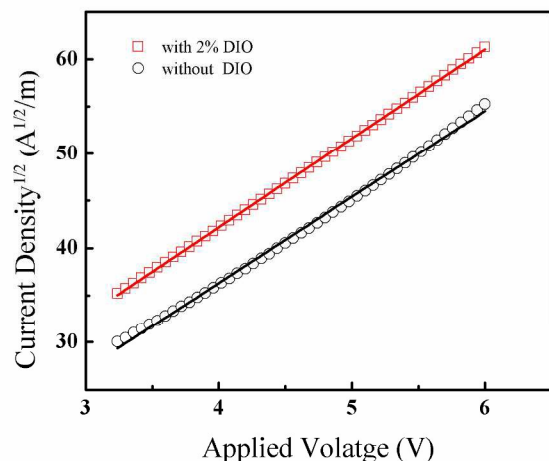


Figure 7. Hole mobility characteristics of PBDT-DTTBT/PC₇₁BM (1 : 1) blends with 2% DIO or not.

To further investigate the effect of DIO additive on the photovoltaic properties, the hole mobility was characterized via the space-charge-limited current (SCLC) method.⁵⁸ The calculated mobility values of the devices with 2% DIO or not are $1.82 \times 10^{-4} \text{ cm}^2 \cdot \text{V}^{-1} \cdot \text{S}^{-1}$ and $7.36 \times 10^{-5} \text{ cm}^2 \cdot \text{V}^{-1} \cdot \text{S}^{-1}$, respectively, shown in Figure 7. The higher hole mobility after adding DIO can well explain the improvement of J_{sc} and PCE in solar cells.

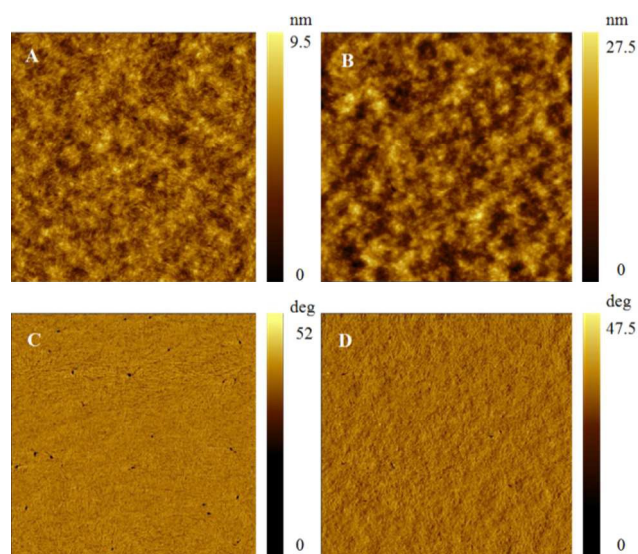


Figure 8. AFM topography (A and B) and phase images (C and D) of the PBDT-DTTBT/PC₇₁BM (1 : 1, w/w) film: (A) without DIO, (B) with 2% DIO (v/v), (C) without DIO, (D) with 2% DIO (v/v). (scan size: $5 \mu\text{m} \times 5 \mu\text{m}$)

The influence of DIO on the morphology of the blend films of PBDT-DTTBT/PC₇₁BM (1 : 1, w/w) were investigated by tapping

mode atomic force microscopy (AFM) and the images are shown in Figure 8. The surface of the blend films without DIO is relative smooth (Figure 8A), corresponding to root-mean-square (RMS) surface roughness of 0.98 nm. The surface topography became rougher after adding 2% DIO (v/v) with a RMS value of 3.82 nm. (Figure 8B) Moreover, the scale of the dark and light domains became obvious (Figure 8C and 8D), implying appropriately enhanced aggregations and proper interpenetrating network formed in the active layer after DIO treatment, which are beneficial for the exciton dissociation and charge carriers transport. This led to a distinct photocurrent improvement of the solar cell devices after DIO treatment (from 9.62 to 12.72 mA/cm^2).^{26, 59, 60} The low crystallinity of the polymer was proved by XRD. (Figure S4)

Conclusions

A novel conjugated BDT polymer (PBDT-DTTBT) is prepared by introducing hexylthiophene substituent to the thiophenebridges between BDT units and BT units. The steric hindrance effect from the flanking hexylthiophene groups can make the main chain twisting strongly compared with non-substituted reference polymer PBDT-DTBT. The twist effect can decrease the conjugated degree of the backbone, and a deep HOMO level can be obtained. More interestingly, the torsion does not make the band gap change which ensures a good light harvesting. The DIO optimized PSCs devices show an efficient PCE of 6.19% with a V_{oc} of 0.80 V, which is a high V_{oc} for the same backbone polymer. The work provides an effective method to design polymers with a deep HOMO level and low band gap for high V_{oc} PSCs.

Experimental

Materials

All of the chemicals were purchased from J&K Scientific and other commercial sources. The reagents and solvents were used as received without further purification, except for tetrahydrofuran (THF) and toluene was dried over Na/benzophenoneketyl and freshly distilled prior to use. 2-Bromo-5-hexylthiophene (Compound 1), 5-hexyl-2,3'-bithiophene (Compound 2), tributyl(5-hexyl-[2,3'-bithiophen]-5'-yl)stannane (Compound 3) and BDT-Sn were synthesized according to the previously reported literature (Scheme 1).^{39, 43, 44} 4,7-Bis(5hexyl[2,3'bithiophen]5'yl)-benzo[c][1,2,5]-thiadiazole (Compound 4), 4,7-bis(2'-bromo-5-hexyl-[2,3'-bithiophen]-5'-yl)Benzo-[c][1,2,5]thiadiazole (DTTBT) and PBDT-DTTBT were synthesized according to Scheme 1. Synthetic details are described below.

Characterization

^1H and ^{13}C NMR (Nuclear magnetic resonance) spectra were recorded on a Bruker Advance III 600 (600 MHz) with tetramethylsilane (TMS) as an internal standard. The molecular weights of the polymers were measured by GPC using THF as the solvent and polystyrene as the standard under 40 °C. TGA was performed on a SDT Q600 with a heating rate of 10 °C/min under a nitrogen atmosphere. UV-vis absorption spectra were recorded by Hitachi U-4100 spectrophotometer. CV measurements were performed on a CHI660D electrochemical workstation under an argon atmosphere in a solution of Bu_4NPF_6 (0.1 M) in acetonitrile at a scan rate of 50 mVs^{-1} at ambient temperature with a Pt working electrode, a Pt wire counter electrode and an SCE reference electrode. DFT calculations were carried out by the Gaussian 09 program suite at the B3LYP/6-31G(d,p) level in the gas phase. The optimized molecular geometries were confirmed to be minimum-energy conformations by computing vibrational frequencies at the same level. Surface morphological characterizations of the films were characterized by a tapping-mode atomic force microscope (AFM, Agilent 5400). The XRD spectrum was obtained on a Hitachi S-4800.

Photovoltaic Device Fabrication

The solar cell devices were fabricated with a structure of ITO/PEDOT:PSS/PBDT-DTTBT:PC₇₁BM/Ca/Al on 15 mm×15 mm patterned indium tin oxide (ITO) coated glass substrates. The ITO glass was cleaned in an ultrasonic bath with acetone, toluene, methanol and isopropyl alcohol sequentially and then an oxygen plasma treatment for 20 min, the substrate was spin-coated with a thin layer of PEDOT:PSS (30 nm) and then dried at 160 °C for 20 min. The active layer was prepared by spin-coating a blend solution of PBDT-DTTBT and PC₇₁BM (30 mg/mL) with different weight ratios in DIO/DCB (0%, 1%, 2%, 3%, or 4% v/v) solution onto the ITO/PEDOT:PSS electrode. Then, the Ca/Al cathode was deposited on the active layer by vacuum evaporation under 3×10^{-4} Pa. The current density-voltage (J - V) characteristics were measured with a Keithley 2420 source measurement unit under simulated 100 mW/cm^2 (AM 1.5 G) irradiation from a Newport solar simulator. Light intensity was calibrated with a standard silicon solar cell. The thickness of the active layer was determined by Dektak 150 profilometer. The EQE of solar cells were analyzed using a certified Newport incident photon conversion efficiency (IPCE) measurement system.

Synthesis of compound 4

Under an argon atmosphere, compound 3 (6 mmol, 3.24 g), 4,7-dibromobenzo[c][1,2,5]thiadiazole (2 mmol, 588 mg) and $\text{Pd}(\text{PPh}_3)_2\text{Cl}_2$ (0.1 mmol, 78 mg) were put into a 100 mL two-necked round-bottom flask in 10 mL of anhydrous toluene. The reactant was refluxed at 80 °C for 24 hours. Then the reaction was quenched with 50 mL of cool water and extracted with chloroform. The organic layer was washed with water and dried over magnesium sulfate. And then the crude product was got by vacuum evaporation and purified by silica gel column chromatography using petroleum ether:dichloromethane (5:1) eluent to obtain the target compound 4 (0.82 g, yield 65%) as a red

solid. ^1H NMR (600 MHz, CDCl_3): δ (ppm) 8.33 (d, 2H, $J=1.33\text{Hz}$ ArH), 7.93 (s, 2H ArH), 7.44 (d, 2H, $J=1.31\text{Hz}$ ArH), 7.15 (d, 2H ArH), 6.77 (d, 2H ArH), 2.86 (t, 4H CH_2), 1.77-1.72 (m, 4H CH_2), 1.46-1.41 (m, 4H CH_2), 1.37-1.35 (m, 8H CH_2), 0.94 (t, 6H CH_3). (Figure S5)

Synthesis of DTTBT

Compound 4 (1.27 g, 2 mmol) was dissolved in 60 mL of chloroform and ethyl acetate (v/v, 4:1), and NBS (392 mg, 2.2 mmol) was added in small portions. The reactant was stirred at room temperature for 10 min, and then 50 mL water was poured into the reaction mixture. After extracted with chloroform, the organic layer was washed with water and dried over magnesium sulfate. The crude product was got by vacuum evaporation and purified by silica gel column chromatography using petroleum ether:dichloromethane (5:1) as eluent, then recrystallized from isopropanol. DTTBT monomer (1.42 g, yield 90%) was obtained after dried under vacuum at 50 °C overnight. ^1H NMR (600 MHz, CDCl_3): δ (ppm) 8.04 (s, 2H ArH), 7.77 (s, 2H ArH), 7.39 (d, 2H ArH), 6.82 (d, 2H ArH), 2.87 (t, 4H CH_2), 1.78-1.73 (m, 4H CH_2), 1.47-1.42 (m, 4H CH_2), 1.38-1.36 (m, 8H CH_2), 0.94 (t, 6H CH_3). ^{13}C NMR (150 MHz, CDCl_3): δ (ppm) 152.10 146.42 138.80 135.30 133.79 127.57 126.11 125.06 124.96 124.33 109.42 31.63 31.62 30.18 28.88 22.62 14.12. (Figure S6 and S7)

Synthesis of PBDT-DTTBT

In a 50 mL two-neck flask, DTTBT monomer (158 mg, 0.2 mmol), BDT-Sn (222 mg, 0.2 mmol), $\text{Pd}_2(\text{dba})_3$ (1.86 mg, 0.002 mmol) and $\text{P}(o\text{-tol})_3$ (3.6 mg, 0.012 mmol) were dissolved in 5 mL of anhydrous toluene. Then the mixture was stirred and purged with argon for 30 min and vigorously stirred at 80°C for 48 h under argon. After cooling down to room temperature, the solution was added dropwise to methanol and filtered. The crude product then was subjected to Soxhlet extraction with methanol and hexane for 24 hours, respectively. Finally, the polymer was purified by silica gel column chromatography (80-100 mesh), and dried under vacuum. PBDT-DTTBT 148 mg, Yield: 51%. ^1H NMR (600 MHz, CDCl_3): δ (ppm) 8.22-6.35 (br 10H), 4.29-3.39 (br 4H), 3.09-2.62 (br 4H), 1.98-1.65 (br 6H), 1.51-1.01 (br, 76H), 0.96-0.74 (br18H). (Figure S8)

Acknowledgements

The authors gratefully acknowledge financial support from the NSFC (21274134, 21274161, 51173199 and 61107090), the Ministry of Science and Technology of China (2010DFA52310), New Century Excellent Talents in University (NCET-11-0473).

Notes

^a Institute of Material Science and Engineering, Ocean University of China, Qingdao 266100, People's Republic of China. Fax: 86-532-66781927; Tel: 86-532-66781690; E-mail: mlsun@ouc.edu.cn

^b CAS Key Laboratory of Bio-based Materials, Qingdao Institute of Bioenergy and Bioprocess Technology, Chinese Academy of Sciences, Qingdao 266101, People's Republic of China. Fax: 86-532-80662778; Tel: 86-532-80662700; E-mail: yangrq@qibebt.ac.cn

‡J. Ren and X. Bao contributed equally to this work.

References

- G. Li, R. Zhu and Y. Yang, *Nat. Photonics*, 2012, **6**, 153.
- Z. He, C. Zhong, S. Su, M. Xu, H. Wu and Y. Cao, *Nat. Photonics*, 2012, **6**, 591.
- B. C. Thompson and J. M. Frechet, *Angew. Chem., Int. Ed.*, 2008, **47**, 58.
- W. Li, S. Albrecht, L. Yang, S. Roland, J. R. Tumbleston, T. McAfee, L. Yan, M. A. Kelly, H. Ade, D. Neher and W. You, *J. Am. Chem. Soc.*, 2014, **136**, 15566.
- L. Ye, S. Zhang, W. Zhao, H. Yao and J. Hou, *Chem. Mater.*, 2014, **26**, 3603.
- S. Zhang, L. Ye, W. Zhao, D. Liu, H. Yao and J. Hou, *Macromolecules*, 2014, **47**, 4653.
- S. H. Liao, H. J. Jhuo, Y. S. Cheng and S. A. Chen, *Adv. Mater.*, 2013, **25**, 4766.
- S. Liu, K. Zhang, J. Lu, J. Zhang, H. L. Yip, F. Huang and Y. Cao, *J. Am. Chem. Soc.*, 2013, **135**, 15326.
- J. You, C. C. Chen, Z. Hong, K. Yoshimura, K. Ohya, R. Xu, S. Ye, J. Gao, G. Li and Y. Yang, *Adv. Mater.*, 2013, **25**, 3973.
- J. You, L. Dou, K. Yoshimura, T. Kato, K. Ohya, T. Moriarty, K. Emery, C. C. Chen, J. Gao, G. Li and Y. Yang, *Nat. Commun.*, 2013, **4**, 1446.
- S. Zhang, L. Ye, W. Zhao, B. Yang, Q. Wang and J. Hou, *Sci. China: Chem.*, 2015, **58**, 248.
- W. Lee, H. Choi, S. Hwang, J. Y. Kim and H. Y. Woo, *Chem. -Eur. J.*, 2012, **18**, 2551.
- Y. Li, *Acc. Chem. Res.*, 2012, **45**, 723.
- L. Yang, H. Zhou and W. You, *J. Phys. Chem. C*, 2010, **114**, 16793.
- Q. Peng, X. Liu, D. Su, G. Fu, J. Xu and L. Dai, *Adv. Mater.*, 2011, **23**, 4554.
- W. Li, W. S. Roelofs, M. M. Wienk and R. A. Janssen, *J. Am. Chem. Soc.*, 2012, **134**, 13787.
- Y. J. Cheng, S. H. Yang and C. S. Hsu, *Chem. Rev.*, 2009, **109**, 5868.
- L. Wang, D. Cai, Q. Zheng, C. Tang, S.-C. Chen and Z. Yin, *ACS Macro Lett.*, 2013, **2**, 605.
- Z. G. Zhang and J. Wang, *J. Mater. Chem.*, 2012, **22**, 4178.
- L. Dou, W. H. Chang, J. Gao, C. C. Chen, J. You and Y. Yang, *Adv. Mater.*, 2013, **25**, 825.
- S. A. Jenekhe, L. Lu and M. M. Alam, *Macromolecules*, 2001, **34**, 7315.
- X. Xu, Y. Wu, J. Fang, Z. Li, Z. Wang, Y. Li and Q. Peng, *Chem. -Eur. J.*, 2014, **20**, 13259.
- M. Wang, H. Wang, T. Yokoyama, X. Liu, Y. Huang, Y. Zhang, T. Q. Nguyen, S. Aramaki and G. C. Bazan, *J. Am. Chem. Soc.*, 2014, **136**, 12576.
- J. Hou, H. Y. Chen, S. Zhang, R. I. Chen, Y. Yang, Y. Wu and G. Li, *J. Am. Chem. Soc.*, 2009, **131**, 15586.
- M. C. Scharber, D. Mühlbacher, M. Koppe, P. Denk, C. Waldauf, A. J. Heeger and C. J. Brabec, *Adv. Mater.*, 2006, **18**, 789.
- J. Wang, M. Xiao, W. Chen, M. Qiu, Z. Du, W. Zhu, S. Wen, N. Wang and R. Yang, *Macromolecules*, 2014, **47**, 7823.
- Y. Dong, X. Hu, C. Duan, P. Liu, S. Liu, L. Lan, D. Chen, L. Ying, S. Su, X. Gong, F. Huang and Y. Cao, *Adv. Mater.*, 2013, **25**, 3683.
- J. Warman, C. Cabanetos, R. Bude, A. El Labban, L. Li and P. M. Beaujuge, *Chem. Mater.*, 2014, **26**, 2829.
- H. Zhou, L. Yang, S. Stoneking and W. You, *ACS Appl. Mater. Interfaces*, 2010, **2**, 1377.
- S. C. Price, A. C. Stuart, L. Yang, H. Zhou and W. You, *J. Am. Chem. Soc.*, 2011, **133**, 4625.
- L. Huo, J. Hou, S. Zhang, H. Y. Chen and Y. Yang, *Angew. Chem., Int. Ed.*, 2010, **49**, 1500.
- J. W. Park, D. H. Lee, D. S. Chung, D.-M. Kang, Y.-H. Kim, C. E. Park and S.-K. Kwon, *Macromolecules*, 2010, **43**, 2118.
- M. Berggren, G. Gustafsson, O. Inganäs, M. R. Andersson, O. Wennerström and T. Hjertberg, *Adv. Mater.*, 1994, **6**, 488.
- M. R. Andersson, M. Berggren, O. Inganaes, G. Gustafsson, J. C. Gustafsson-Carlberg, D. Selse, T. Hjertberg and O. Wennerstroem, *Macromolecules*, 1995, **28**, 7525.
- C. P. Chen and H. L. Hsu, *Macromol. Rapid. Comm.*, 2013, **34**, 1623.
- Q. Liu, X. Bao, S. Wen, Z. Du, L. Han, D. Zhu, Y. Chen, M. Sun and R. Yang, *Polym. Chem.*, 2014, **5**, 2076.
- E. Zhou, J. Cong, K. Hashimoto and K. Tajima, *Macromolecules*, 2013, **46**, 763.
- Y. Li, Y. Chen, X. Liu, Z. Wang, X. Yang, Y. Tu and X. Zhu, *Macromolecules*, 2011, **44**, 6370.
- X. Wang, Y. Sun, S. Chen, X. Guo, M. Zhang, X. Li, Y. Li and H. Wang, *Macromolecules*, 2012, **45**, 1208.
- B. Qu, H. Yang, D. Tian, H. Liu, Z. Cong, C. Gao, Z. Chen, L. Xiao, Z. Gao, W. Wei and Q. Gong, *Synth. Met.*, 2012, **162**, 2020.
- N. Wang, Z. Chen, W. Wei and Z. Jiang, *J. Am. Chem. Soc.*, 2013, **135**, 17060.
- Y. Huang, F. Liu, X. Guo, W. Zhang, Y. Gu, J. Zhang, C. C. Han, T. P. Russell and J. Hou, *Adv. Energy Mater.*, 2013, **3**, 930.
- T. V. Richter, C. H. Braun, S. Link, M. Scheuble, E. J. W. Crossland, F. Stelzl, U. Würfel and S. Ludwigs, *Macromolecules*, 2012, **45**, 5782.
- T. Cai, Y. Zhou, E. Wang, S. Hellström, F. Zhang, S. Xu, O. Inganäs and M. R. Andersson, *Sol. Energy Mater. So. Cells*, 2010, **94**, 1275.
- D. Ouyang, M. Xiao, D. Zhu, W. Zhu, Z. Du, N. Wang, Y. Zhou, X. Bao and R. Yang, *Polym. Chem.*, 2014, **6**, 55.
- H.-C. Chen, Y.-H. Chen, C.-C. Liu, Y.-C. Chien, S.-W. Chou and P.-T. Chou, *Chem. Mater.*, 2012, **24**, 4766.
- Y.-J. Cheng, C.-H. Chen, Y.-S. Lin, C.-Y. Chang and C.-S. Hsu, *Chem. Mater.*, 2011, **23**, 5068.
- L. Han, X. Bao, T. Hu, Z. Du, W. Chen, D. Zhu, Q. Liu, M. Sun and R. Yang, *Macromol. Rapid. Comm.*, 2014, **35**, 1153.
- J. J. Intemann, K. Yao, Y.-X. Li, H.-L. Yip, Y.-X. Xu, P.-W. Liang, C.-C. Chueh, F.-Z. Ding, X. Yang, X. Li, Y. Chen and A. K. Y. Jen, *Adv. Funct. Mater.*, 2014, **24**, 1465.
- X. Wang, P. Jiang, Y. Chen, H. Luo, Z. Zhang, H. Wang, X. Li, G. Yu and Y. Li, *Macromolecules*, 2013, **46**, 4805.
- Y. Li, Y. Cao, J. Gao, D. Wang, G. Yu and A. J. Heeger, *Synth. Met.*, 1999, **99**, 243.
- H. Zhang, L. Ye and J. Hou, *Polym. Int.*, 2015. DOI: 10.1002/pi.4895
- S. Gunes, H. Neugebauer and N. S. Sariciftci, *Chem. Rev.*, 2007, **107**, 1324.
- J. Peet, M. L. Senatore, A. J. Heeger and G. C. Bazan, *Adv. Mater.*, 2009, **21**, 1521.
- J. K. Lee, W. L. Ma, C. J. Brabec, J. Yuen, J. S. Moon, J. Y. Kim, K. Lee, G. C. Bazan and A. J. Heeger, *J. Am. Chem. Soc.*, 2008, **130**, 3619.
- F. S. Kim, X. Guo, M. D. Watson and S. A. Jenekhe, *Adv. Mater.*, 2010, **22**, 478.
- D. Veldman, S. C. J. Meskers and R. A. J. Janssen, *Adv. Funct. Mater.*, 2009, **19**, 1939.
- V. Mihailetchi, J. Wildeman and P. Blom, *Phys. Rev. Lett.*, 2005, **94**, 126602.
- G. Ren, E. Ahmed and S. A. Jenekhe, *Adv. Energy Mater.*, 2011, **1**, 946.
- W. Chen, Z. Du, L. Han, M. Xiao, W. Shen, T. Wang, Y. Zhou and R. Yang, *J. Mater. Chem. A*, 2015, **3**, 3130.